AD-A143 384 POINT RESPONSE FUNCTIONS FOR UNFILLED OPTICAL ARRAYS 1/1
(U) NAVAL RESEARCH LAB WASHINGTON DC
J H SPENCER ET AL. 27 JUL 84 NRL-MR-5355

UNCLASSIFIED F/G 20/6 NL

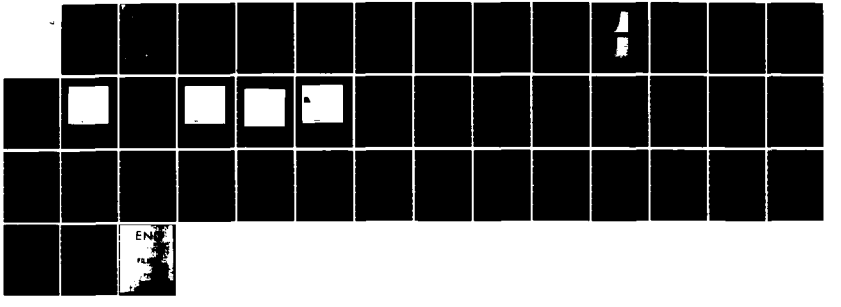

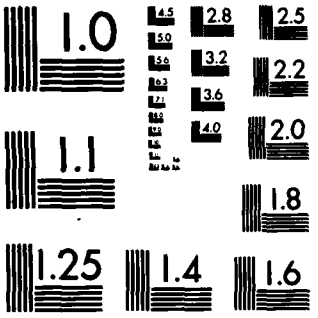

NRL Memorandum Report 5355

Point Response Functions for Unfilled Optical Arrays

J.H. SPENCER AND R.S. SIMON

Radio and IR Astronomy Branch
Space Science Division

July 27, 1984

NAVAL RESEARCH LABORATORY
Washington, D.C.

SECURITY CLASSIFICATION OF THIS PAGE

REPORT DOCUMENTATION PAGE

1a REPORT SECURITY CLASSIFICATION UNCLASSIFIED	1b RESTRICTIVE MARKINGS
2a SECURITY CLASSIFICATION AUTHORITY	3 DISTRIBUTION/AVAILABILITY OF REPORT Approved for public release; distribution unlimited.
2b DECLASSIFICATION/DOWNGRADING SCHEDULE	
4 PERFORMING ORGANIZATION REPORT NUMBER(S) NRL Memorandum Report 5355	5. MONITORING ORGANIZATION REPORT NUMBER(S)
6a NAME OF PERFORMING ORGANIZATION Naval Research Laboratory 6b OFFICE SYMBOL (If applicable) Code 4130	7a. NAME OF MONITORING ORGANIZATION
6c ADDRESS (City, State and ZIP Code) Washington, DC 20375	7b. ADDRESS (City, State and ZIP Code)
8a. NAME OF FUNDING/SPONSORING ORGANIZATION Office of Naval Research 8b OFFICE SYMBOL (If applicable)	9. PROCUREMENT INSTRUMENT IDENTIFICATION NUMBER
8c ADDRESS (City, State and ZIP Code) Arlington, VA 22217	10 SOURCE OF FUNDING NOS. PROGRAM ELEMENT NO. 61153N; PROJECT NO. RR034-06-41; TASK NO.; WORK UNIT NO DN880-099
11 TITLE (Include Security Classification) Point Response Functions for Unfilled Optical Arrays	
12 PERSONAL AUTHOR(S) Spencer, J.H. and Simon, R.S.	
13a TYPE OF REPORT Interim 13b TIME COVERED FROM TO	14. DATE OF REPORT (Yr., Mo., Day) July 27, 1984 15 PAGE COUNT 43
16. SUPPLEMENTARY NOTATION	
17 COSATI CODES FIELD / GROUP / SUB. GR.	18. SUBJECT TERMS (Continue on reverse if necessary and identify by block number) Optical, Modulation function, Imaging Array, Point response, Image processing

19 ABSTRACT (Continue on reverse if necessary and identify by block number)

Two problems relating to the design of arrays for imaging complex fields are the sidelobe levels and the energy within those sidelobes. While designers often know the performance of a filled aperture, the much larger number of parameters involved in array design lead to great difficulty evaluating the performance level. This report describes a family of optical arrays whose parameters were evaluated by a computer analysis system. For simplicity all the arrays considered were in the same family (a circular ring of evenly spaced array elements), so that comparisons could be made as the number of array elements was varied. Arrays with 3, 7, 15, and 27 elements were considered in detail, including the proper corrections for both finite elementsize and finite bandpass.

We conclude that a spaceborne, unfilled, minimum-redundancy array can be built for earth viewing that has performance similar to a filled aperture significantly reducing the cost of space based imaging systems.

(Continues)

20 DISTRIBUTION/AVAILABILITY OF ABSTRACT UNCLASSIFIED/UNLIMITED ☒ SAME AS RPT ☐ OTIC USERS ☐	21 ABSTRACT SECURITY CLASSIFICATION UNCLASSIFIED
22a NAME OF RESPONSIBLE INDIVIDUAL J. H. Spencer	22b TELEPHONE NUMBER (Include Area Code) (202) 767-3050 22c OFFICE SYMBOL Code 4130

DD FORM 1473, 83 APR EDITION OF 1 JAN 73 IS OBSOLETE

SECURITY CLASSIFICATION OF THIS PAGE

19. ABSTRACT (Continued)

The sidelobe levels and energy in the sidelobes can be controlled through the appropriate selection of design parameters. However a final, detailed design will depend upon target characteristics and cost-benefit tradeoffs, as well as upon the center wavelength, bandpass, desired resolution, and the allowable sidelobe levels. The analysis methods we have developed have general applicability to the design problem.

CONTENTS

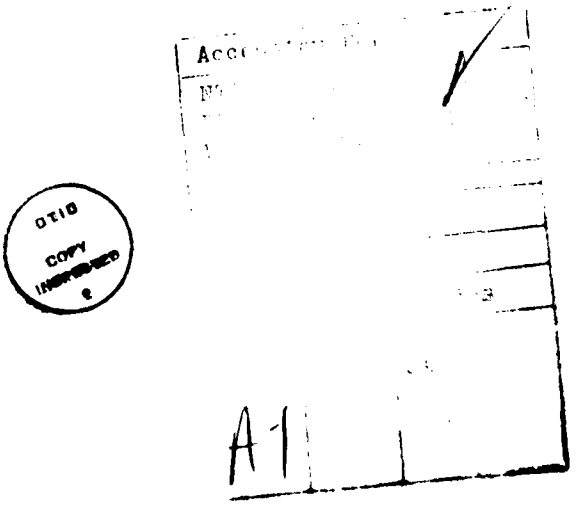

POINT RESPONSE FUNCTIONS FOR UNFILLED OPTICAL ARRAYS

ABSTRACT

Two problems relating to the design of arrays for imaging complex fields are the sidelobe levels and the energy within those sidelobes. While designers often know the performance of a filled aperture, the much larger number of parameters involved in array design lead to great difficulty evaluating the performance level. This report describes a family of optical arrays whose parameters were evaluated by a computer analysis system. For simplicity all the arrays considered were in the same family (a circular ring of evenly spaced array elements), so that comparisons could be made as the number of array elements was varied. Arrays with 3, 7, 15, and 27 elements were considered in detail, including the proper corrections for both finite element size and finite bandpass.

We conclude that a spaceborne, unfilled, minimum-redundancy array can be built for earth viewing that has performance similar to a filled aperture significantly reducing the cost of space based imaging systems. The sidelobe levels and energy in the sidelobes can be controlled through the appropriate selection of design parameters. However a final, detailed design will depend upon target characteristics and cost-benefit tradeoffs, as well as upon the center wavelength, bandpass, desired resolution, and the allowable sidelobe levels. The analysis methods we have developed have general applicability to the design problem.

INTRODUCTION

The use of interferometer systems in applications where they previously could not be used is now possible because of great advances in both interferometer and image processing techniques in the past decade. This is partially due to better signal processing hardware and software and because imaging problems arose which needed novel solutions. While interferometers provide increased resolution at low cost, their increased sidelobe levels can create major problems, especially for an imaging system. In a simple field where the received signal is localized to a small percentage of the total image, high sidelobes can be tolerated and elementary methods restore the original brightness distribution satisfactorily. However, in the case of a down-looking system from high altitudes or space, the image brightness is complicated; there is information in every part of the image, much of which is irrelevant and must be removed to recognize a target. Removing the background is almost impossible if the point response function of the system has high sidelobes extending across the image, because objects are not localized. We describe an optical array that has low sidelobe levels and a high percentage of the power in the main beam.

Of possible greater importance, this technical memorandum also describes a new computer analysis system for examining the sidelobe levels and their effect upon an image. A family of spaceborne optical arrays have been examined to demonstrate these techniques. It should be emphasized that there is nothing special in the demonstration array. Using this analysis system, a completely different configuration could be thoroughly examined with a few weeks of work.

Manuscript approved March 12, 1984.

Radio astronomers are not able to build filled apertures to achieve the resolution they desire. Since adequate sensitivity can be achieved with an unfilled aperture, they have built interferometer systems (ref. 1, 2). They have had the problem of high sidelobes for many years because of practical limits to the number of elements in any array. As a result, extensive software has been developed for calculating point response functions for realistic cases using arbitrarily located elements. The basic approach of this memorandum is therefore to apply some of these special computer programs to the specific case of an optical array, writing new programs to aid the interfacing or to do peculiar cases.

We first review the optical theory which leads to the point response function of addition correlators. This is a different situation from the more familiar multiplication correlators used at radio wavelengths. Before examining complex interferometers, the radial distribution of the point response function for a filled aperture is derived and compared to a circularly symmetric interferometer. Finally the discrete element broad bandpass case is synthesized.

THE THEORY OF ADDITION CORRELATORS

The first step in understanding optical interferometers is to review the physics of addition correlators. At the present it is not technically possible to make multiplying optical interferometers similar to conventional radio interferometers. Following the basic development of Born and Wolf (ref. 3), we see that for a plane wave the total intensity is related to the electric vector by:

$$I = \frac{c}{4\pi}\sqrt{\frac{\varepsilon}{\mu}}\ \langle \vec{E}^2 \rangle \tag{1}$$

where the electric vector, $\vec{E}(\vec{r},t) = \mathrm{Re}\ \{A(\vec{r})e^{-i\omega t}\}$, is a function of space and time. Now consider the superposition of two monochromatic waves $\vec{E}_1$ and $\vec{E}_2$ at a point in space, P

$$\vec{E} = \vec{E}_1 + \vec{E}_2$$

or

$$\langle \vec{E}^2 \rangle = \langle \vec{E}_1^{\,2} \rangle + \langle \vec{E}_2^{\,2} \rangle + 2 \langle \vec{E}_1 \cdot \vec{E}_2 \rangle \tag{2}$$

Hence the total intensity, I, at point P is

$$I = I_1 + I_2 + J_{12} \tag{3}$$

where we have made use of the definitions

$$I_1 = \langle \vec{E}_1^{\,2} \rangle \ ; \ I_2 = \langle \vec{E}_2^{\,2} \rangle ; \ J_{12} = 2 \langle \vec{E}_1 \cdot \vec{E}_2 \rangle \quad .$$

Notice that the intensities I_1, I_2, and I are positive definite by this formulation, but no such requirement exists for J_{12}. Radio astronomers are able to measure the interference term J_{12} separately in eq. 3 because they use a multiplication correlator instead of the addition correlator as was used in obtaining eq. 3. As a result radio astronomers can obtain negative sidelobes

and negative portions of their images, while that is impossible for the addition correlator.

Expanding this analysis to n elements is relatively easy.

$$I = \langle \vec{E}_1^{\,2} \rangle + \langle \vec{E}_2^{\,2} \rangle + \ldots + \langle \vec{E}_n^{\,2} \rangle + 2 \langle \vec{E}_1 \cdot \vec{E}_2 \rangle + \ldots + 2 \langle \vec{E}_1 \cdot \vec{E}_n \rangle + \ldots + 2 \langle \vec{E}_{n-1} \cdot \vec{E}_n \rangle \quad (4)$$

The sum of all the cross terms J_{mn} divided by the number of cross terms is what radio astronomers call the "synthesized beam". There are standard computer programs for computing the synthesized beam, so it is easy to analyze the characteristics of an optical array using the synthesized beam as a starting point. For an interferometer with n identical elements there are $n(n-1)/2$ cross terms, and eq. 4 simplifies to:

$$I = n\,(I_1 + (n-1)\,[\text{Synthesized Beam}]) \quad (5)$$

This result is for infinitesimally small point interferometer elements and monochromatic waves. For finite elements the equation must be multiplied by the individual element response which is an envelope or gain function for the intensity as given in eq. 5. For a finite bandpass the fringe functions add out of phase so as to apply a taper to the synthesized beam for angles off axis (See Appendix A). Therefore a bandpass effect is applied only to the second term on the right hand side of eq. 5. If we denote the (normalized) response of the individual elements by A(x,y) and the bandpass effect by B(x,y) we obtain,

$$I(x,y) = n\,A(x,y)\,[I_1(x,y) + (n-1)\,B(x,y)\,b(x,y)] \quad (6)$$

where we have finally denoted the synthesized beam by b(x,y). We will be able to examine these terms more closely by using several special cases. A most important special case is when the number of elements approaches infinity and the aperture is filled. This limiting case is examined next.

THE POINT RESPONSE OF A FILLED APERTURE

Interferometers do not measure the brightness of the image directly, but measure the Fourier transform of the image which is the image visibility V(u,v). In the case of a point source at the (x,y) origin, the visibility is a constant vector with zero phase and an amplitude equal to the flux density of the point source. The synthesized beam of an array of interferometers can be written as

$$b(x,y)\ [* *]\ S(u,v)\ w(u,v) \quad (7)$$

where

b(x,y) = synthesized beam.
S(u,v) = sampling function that represents the distribution of the data points in the (u,v) plane.

w(u,v) = weighting function of the data including any applied tapering. S(u,v) w(u,v) is the optical modulation transfer function.
[* *] denotes Fourier transformation.

The function S(u,v)w(u,v) is entirely real so b(x,y) is symmetrical.

In real situations there is finite bandwidth. The mathematics for two element interferometers with finite bandpass and for a simple 5 percent rectangular bandpass array are derived in Appendix A. The two element result is a reduction in the fringe amplitude (reduction in the sidelobe level) as the distance from the delay center increases with the functional relationship of sin(x)/x where this x is π times angular distance divided by baseline. The general case of discrete arrays with large bandpass is not solved in closed form; for the calculations of this report we sum the n(n-1)/2 sin(x)/x terms directly using a computer.

The monochromatic point response function of a circular filled aperture is then simply the Fourier Transform of a uniform disk, the first order Bessel function $J_1(\pi r/a)/(r/a)$ where a is the diameter of the aperture. This radial dependency is shown in Fig. 1 where we have assumed a diameter of 10 meters and a center wavelength of 500 nm. When the effects of the finite rectangular bandpass from 350 nm to 650 nm are taken into account, the point response function is effectively multiplied by the delay response, shown in Fig. 2a. The broadband result is shown in Fig. 2b.

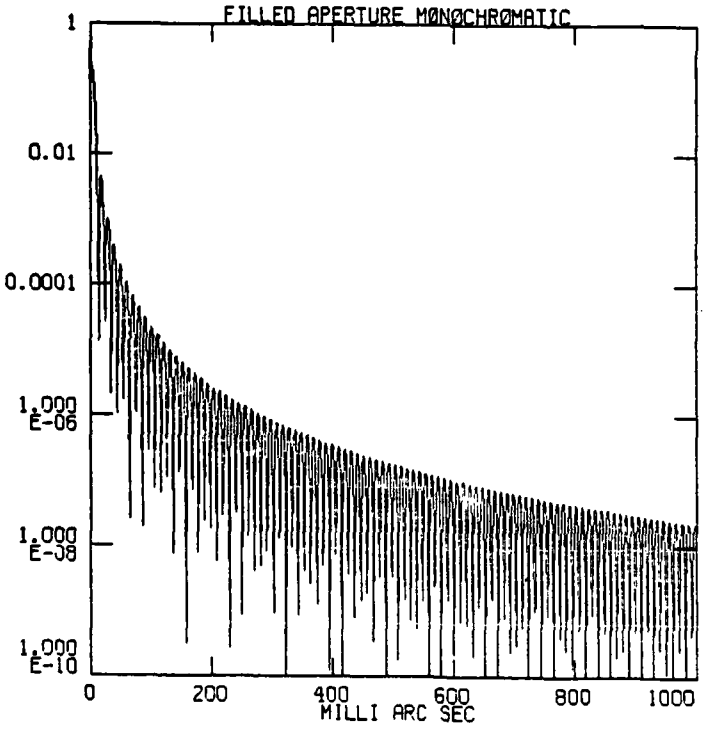

Figure 1. Point response function of a monochromatic filled aperture 5 meters in radius.

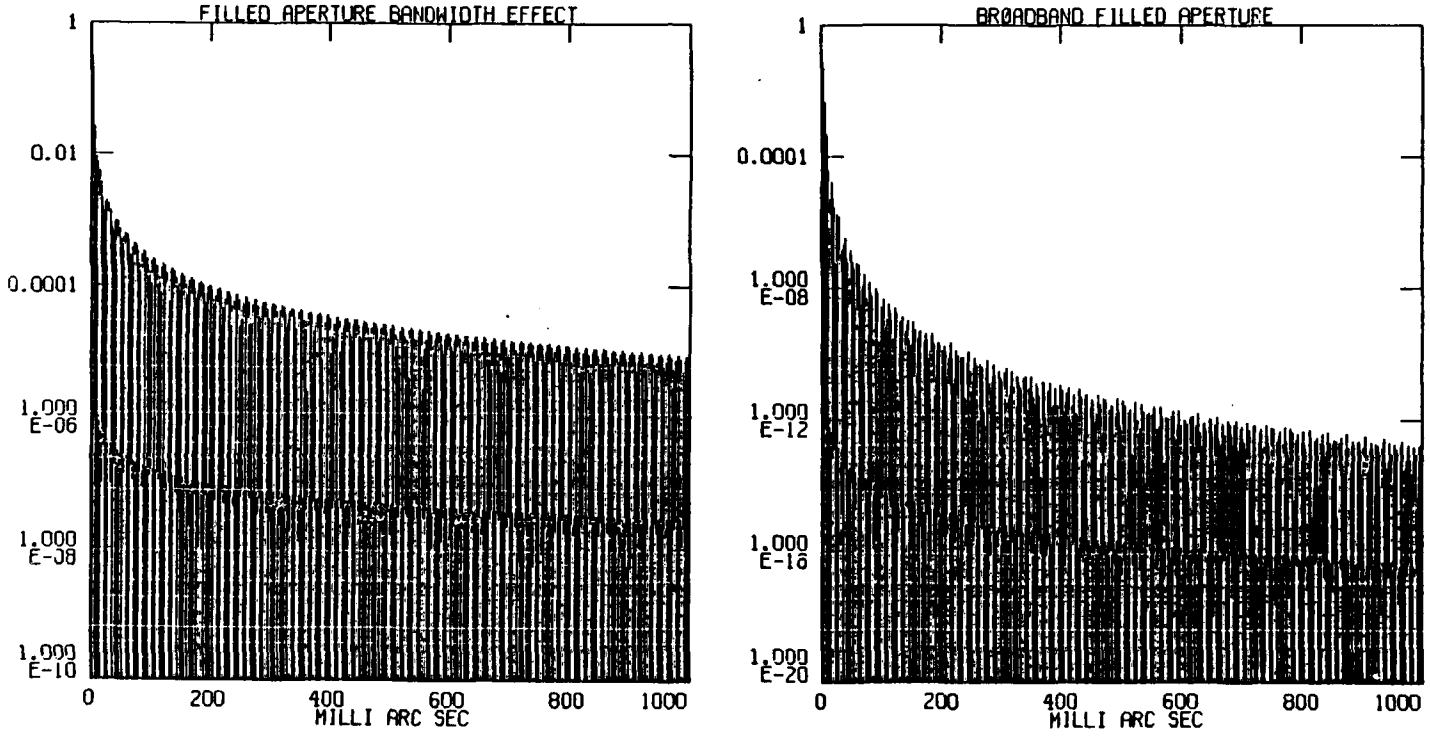

Figure 2. Bandpass effects for the filled aperture. (a) Taper due to a bandpass from 350 nm to 650 nm and a 10 m aperture. (b) Bandpass taper applied to the monochromatic point response function of a filled aperture to obtain the point response function for a finite bandpass.

THE CIRCULARLY SYMMETRIC INTERFEROMETER

We next calculate the results for the case of an infinite number of point elements arranged in a circle. This important case is solvable in closed form (ref. 4) and the synthesized beam b(x,y) is given by

$$b(x,y) = J_o(\pi r/a) \tag{8}$$

where a is used to denote the radius of the circle. This function (shown in Fig. 3) does not decrease with r nearly as rapidly as $J_1(x)/x$ which we found for a filled aperture. However, in realistic cases finite element size and bandpass provide a taper to lower the sidelobe level more rapidly than eq. 8.

Combining eqs. 6 and 8 leads to

$$I(x,y) = A(x,y)\ B(x,y)\ J_o(\pi r/a) \tag{9}$$

because as n approaches infinity the first term of eq. 6 can be neglected. This is the same result as for a multiplication correlator.

At a distance of 1 arcsecond the sidelobes have dropped to 30 dB down from the central maximum, but are 50 dB higher than for the circular aperture case. Because these profiles are well known and understood, it is easy to use spatial filtering to make the ring response match the filled aperture. The matched filter is $[x\ J_o(x)/J_1(x)]^2$.

If the effects of finite element size are included into the profile shown in Fig. 3a, the function drops more rapidly. The 10 cm elements assumed here have a minimum at a full width half maximum of 1 arcsecond. If a single detector is used at each element (as in a radio interferometer), then the finite bandpass response will severely narrow the array response, providing an additional sidelobe suppression. The combined effects of finite elements and bandpass are shown in Fig. 3b.

THE DISCRETE ELEMENT ANALYSIS

The problem of simulating the point response function at the origin of a complex array with finite elements and a broad bandpass is the special case of simulating the response to any image. To allow for more general cases, the best approach is to simulate the array (using software) for a specific array geometry, wavelength, bandpass, etc. We chose a ring geometry for the elements, since that maximizes the two dimensional resolution and yields a reasonable compromise for the minimum element spacing. Thus, a ring is a system with a wide range of spatial frequencies. We analyzed the realistic case of finite circular elements arranged on a ring. We have considered in some detail ring arrays of 3, 4, 7, 9, 15, 27, 45, and 99 elements, but we have not applied the full details of the analysis in all cases. As the number of elements in the ring increases, they are closer spaced, which pushes the first grating ring further out. Within this ring the discrete element case is closely approximated by the infinitesimal ring discussed above.

For our analysis, we have assumed a geometry consisting of a 10 meter array operating at a wavelength of 500 nanometers. The analysis includes both point elements and the more realistic case of 10 cm elements. For broadband

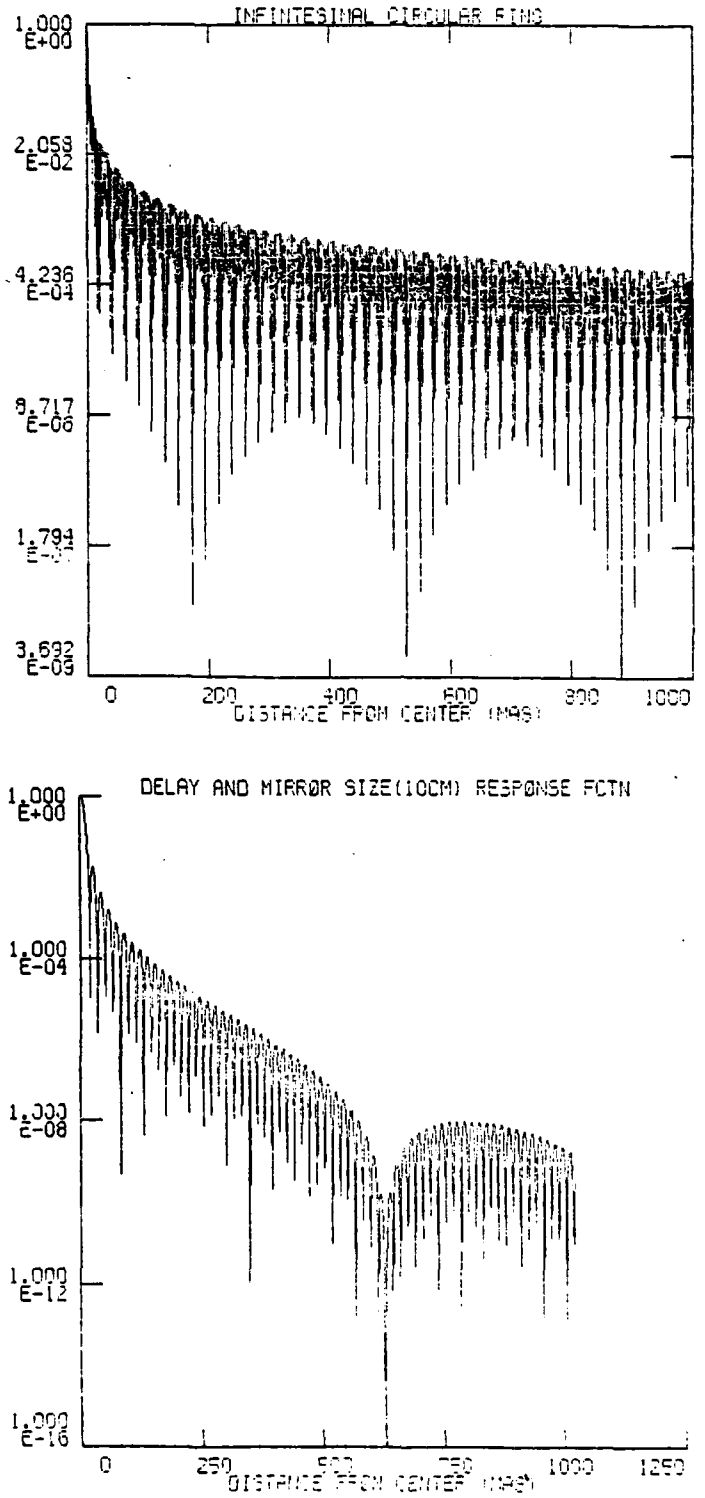

Figure 3. Point response function for the circularly symmetric unfilled aperture. (a)Monochromatic case. (b)Finite bandpass case.

effects we assume a uniform wavelength response between 350 and 650 nanometers. Unless specifically stated however, results are for monochromatic light at 500 nanometers. The analysis assumes the beams from array elements are combined coherently. This assumption implies that the interferometer is built away from the degrading effects of the atmosphere. System noise and other operational degradations are not a part of the point response function, and were not considered. Conceptually, the interferometer we are considering consists of an array of elements on a ring, whose individual beams are brought to a common focus.

The analysis system we have developed is a collection of specialized programs from two different image analysis systems with the addition of a few programs specially written for this project. The basic flow shown in Fig. 4 is to assume an interferometer configuration, generate fake data for it using the Caltech Very Long Baseline Interferometer (VLBI) package (ref. 5), convert the fake data to the NRAO image processing package AIPS (ref. 6), and invert the data to obtain the synthesized beam. This is the synthesized beam for monochromatic point elements. Using the interactive data language IDL (ref. 7), we generate the element responses for the interferometer and convert it into AIPS format where it can be combined with the synthesized beam and plotted in a variety of ways. The bandpass correction function was introduced separately from a special-purpose Fortran program.

Because both of the major packages we use are organically growing at the present time, a detailed step-by-step description of the method would be obsolete when the next release is received within the month. Of more value is a flow description which leads to an understanding for the need for each step. The exact modeling done here is necessarily quite complicated and requires many stages through the software.

The first step in the analysis (see Fig. 4) was to create an artificial interferometer data set, using the Caltech VLBI program FAKE. In appendix B are the 3 files used to run this program in the case of the 15-element array. The parameters in the FAKE.COM file were selected to give a "noise-free" data set symmetric about the V axis in the UV plane. The file STATIONS.DAT contained the element positions; POINT.MOD contained the parameters for a dummy input source model (for the purposes of our analysis, the type of input source model used was irrelevant). The original maps made from the model (using the data generated by FAKE) did not include either bandpass or finite element effects and thus could not be used directly. The model source data is discarded following the UVSRT program step. The elements were located on a circle; for convenience a circle of latitude was used with the frequency being scaled so as to give a circular interferometer with the desired size of 20 million wavelengths. Further explanation of the parameters used for FAKE can be found in the documentation for the Caltech VLBI package (ref. 5).

The fake data was then translated into the AIPS format using the AIPS program TOAIP, (or FRMVB for more than 27 elements), sorted as necessary using UVMAP, and then Fourier transformed by UVMAP. UVMAP has 2 output images: the normalized synthesized beam b(x,y) for the array under consideration and the so-called "dirty-map", the latter of which was discarded. The synthesized beam is the point response function for the monochromatic, point-like element case, with a zero-level offset (see eq. 6). As an example, the synthesized beam b(x,y) for a 15-element array is presented in Fig. 5.

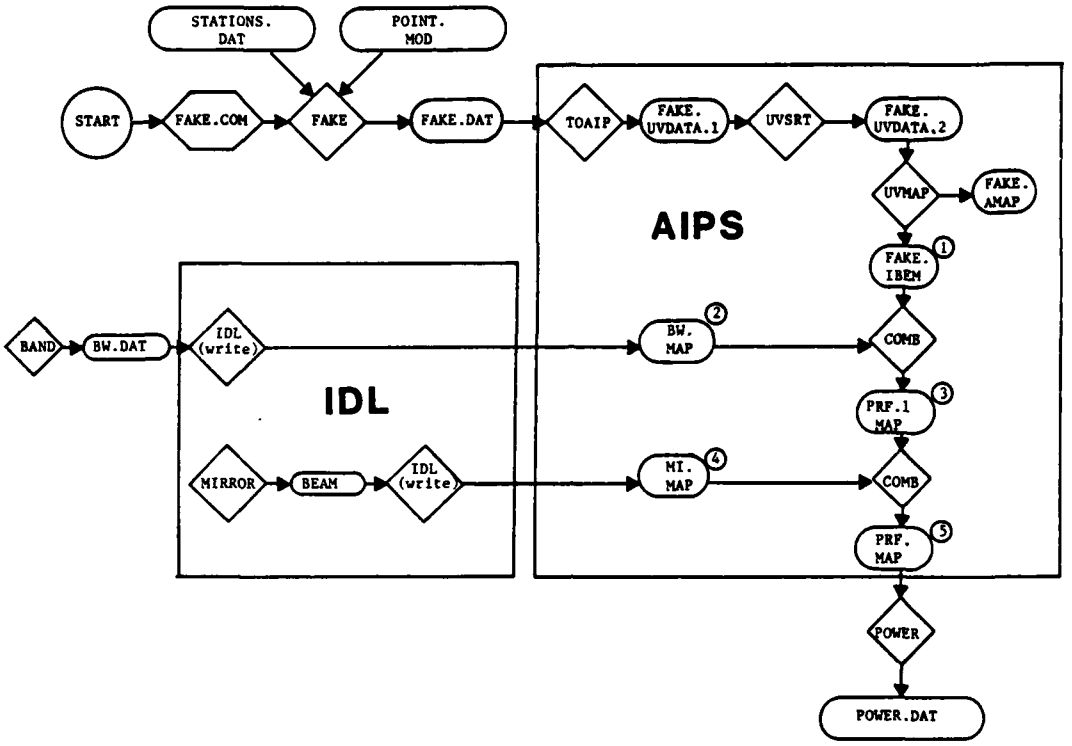

Figure 4. Computer analysis logical flow. The flow chart shows the relationship between the various programs to produce point response functions for finite bandpasses and finite elements. The numbered points on the flow chart refer to intermediate images as follows:

(1) FAKE.IBEM is the monochromatic synthesized beam b(x,y) in equation 6.
(2) BW.MAP is the bandpass correction function B(x,y).
(3) PRF1.MAP is the term [I1(x,y) + n-1 B(x,y) b(x,y)] in equation 6, which represents the normalized point response function for an array of point elements with finite bandpass.
(4) MI.MAP is the term A(x,y) in equation 6, representing the beam from the individual elements in the array.
(5) PRF.MAP is I(x,y), the normalized point response function for finite bandpass and finite element size.

(Page 10 Blank)

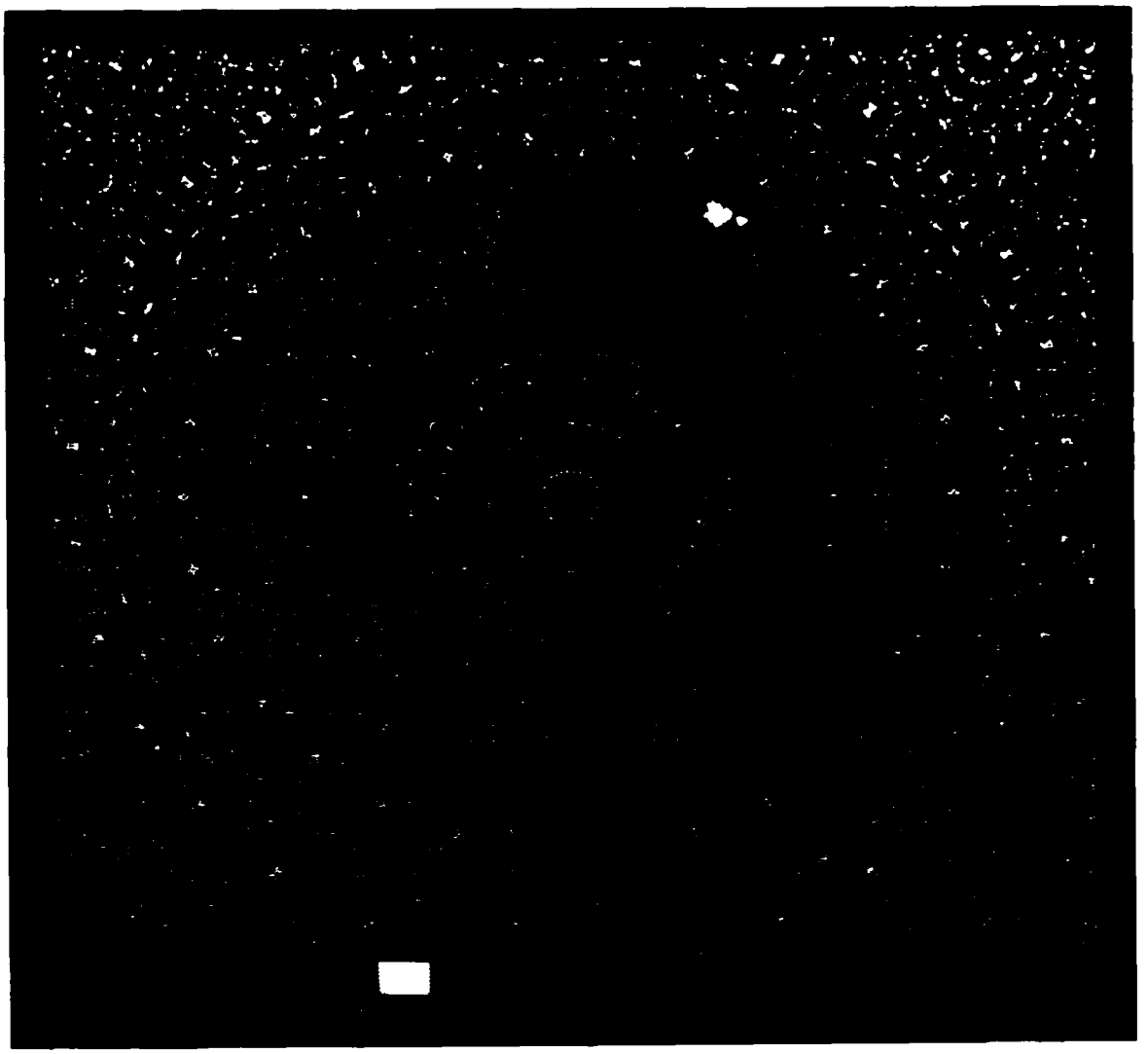

Figure 5. Synthesized beam function for the discrete element unfilled aperture (monochromatic case and point elements). The array consisted of 15 elements arranged on a ring. The scale across the bottom defines color as a function of brightness. This map corresponds to FAKE.IBEM in the flow chart of Fig. 4.

The taper due to the finite bandpass must next be accounted for. For the special case of an odd number of elements arranged symmetrically on a ring, program BAND (Appendix B) generates the bandpass array B(x,y) by which the synthesized beam must be multiplied. For a generalized array with arbitrary element locations, BAND could not be used as it stands, but would have to be modified to read the UV data to get the position angle and scaling for the sin(x)/x calculations. An example of the B(x,y) function for the 15-element array is shown in Fig. 6.

The array from BAND is copied into an existing dummy AIPS image file using IDL for convenience in getting the correct format. To use IDL in this way, one first opens and reads the data file into an internal array in IDL. Next, the AIPS dummy file is opened using an OPENU statement (see the IDL documentation, ref. 7, for details). Next, a variable is associated with the AIPS file. Then the internal array is copied into the associated variable with a statement like A(0)=B. Finally the AIPS file is closed in the standard way. Care must be taken not to corrupt the normalization of the AIPS file too badly, or unpredictable things can happen. Also, IDL must write the file with the correct data type needed by AIPS.

The multiplication of the synthesized beam b(x,y) by the bandpass function B(x,y) is performed by the AIPS task COMB. In the same operation, the (n-1) factor for the product (see eq. 6) is applied and the constant I_1 term in equation (6) is added to produce the intermediate map PRF1. PRF1 is the normalized point response function for an array of point elements having a finite bandpass. PRF1 MAP for the 15-element array is presented in Fig. 7. There is a dramatic improvement in the sidelobe level due to B(x,y).

The final step in producing the point response function is to apply the finite element correction A(x,y). This correction was generated using the IDL procedure MIRROR (see appendix B) and copied into AIPS using IDL (see above). COMB was then used to multiply and renormalize the two arrays resulting in the final image of the point response function for the finite-sized element, finite-passband array. See Fig. 8. It is important to emphasize that the point response functions in Fig. 8 are what a detector array in our "conceptual" interferometer would measure for a point source.

While the point response functions for the type of arrays under consideration are necessarily two dimensional, the high degree of symmetry in the class of arrays we studied means that the average radial dependence of the point response function is of interest. We used the program POWER (listed in Appendix B) to read the AIPS map file and average over azimuth to obtain the profiles shown in Fig. 9. The broad pedestal in each profile is the remnant of the individual response.

In the case of a complex source, the response would be simply the convolution of the point response function we have calculated with the true source. Deconvolution to obtain the maximum possible resolution with high dynamic range is possible.

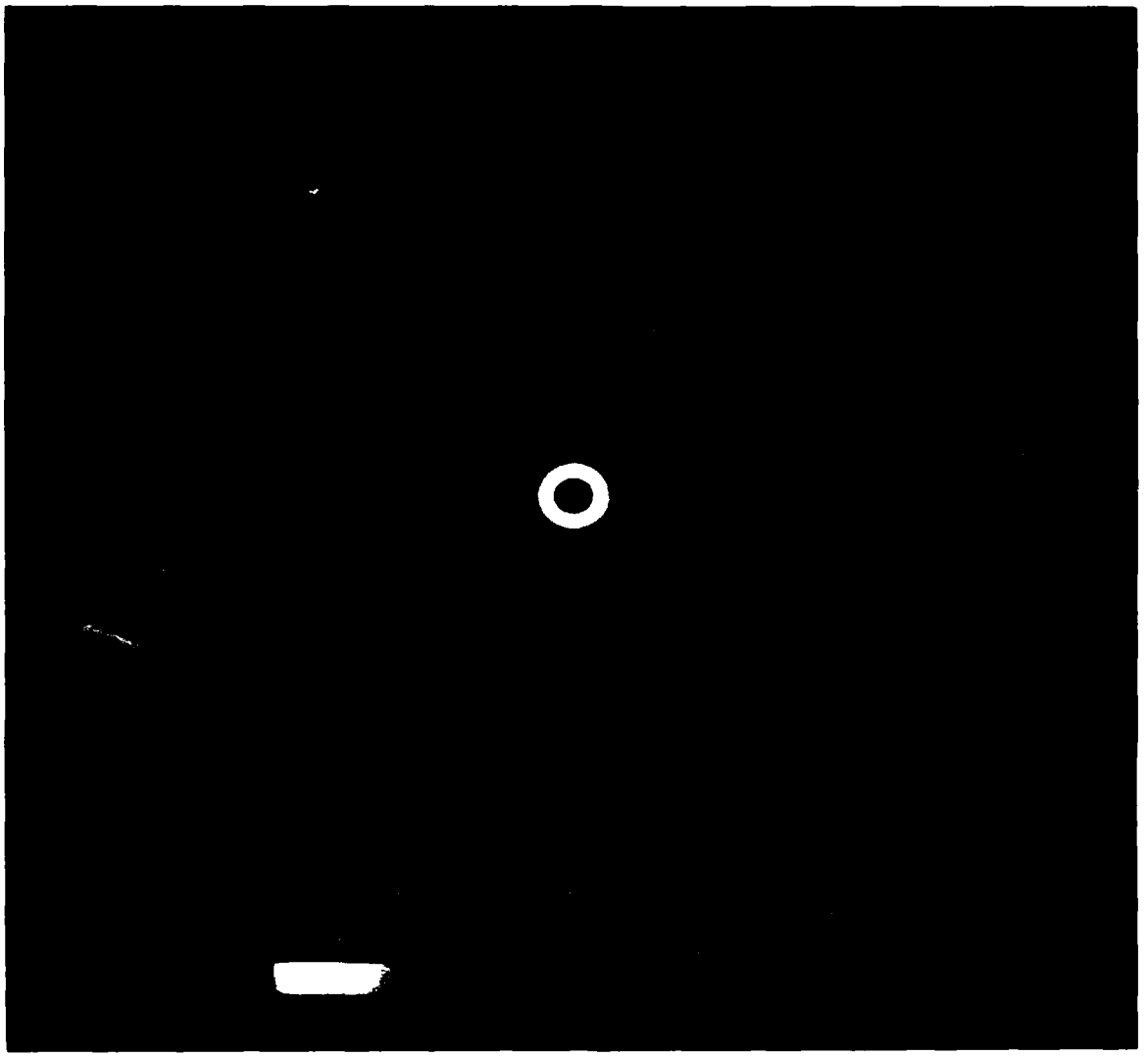

Figure 6. Bandpass correction B(x,y) for the 15 element array considered in detail. This corresponds to BW.MAP in Fig. 4. Note that the color wedge along the bottom has been adjusted to exaggerate the fainter parts of the image.

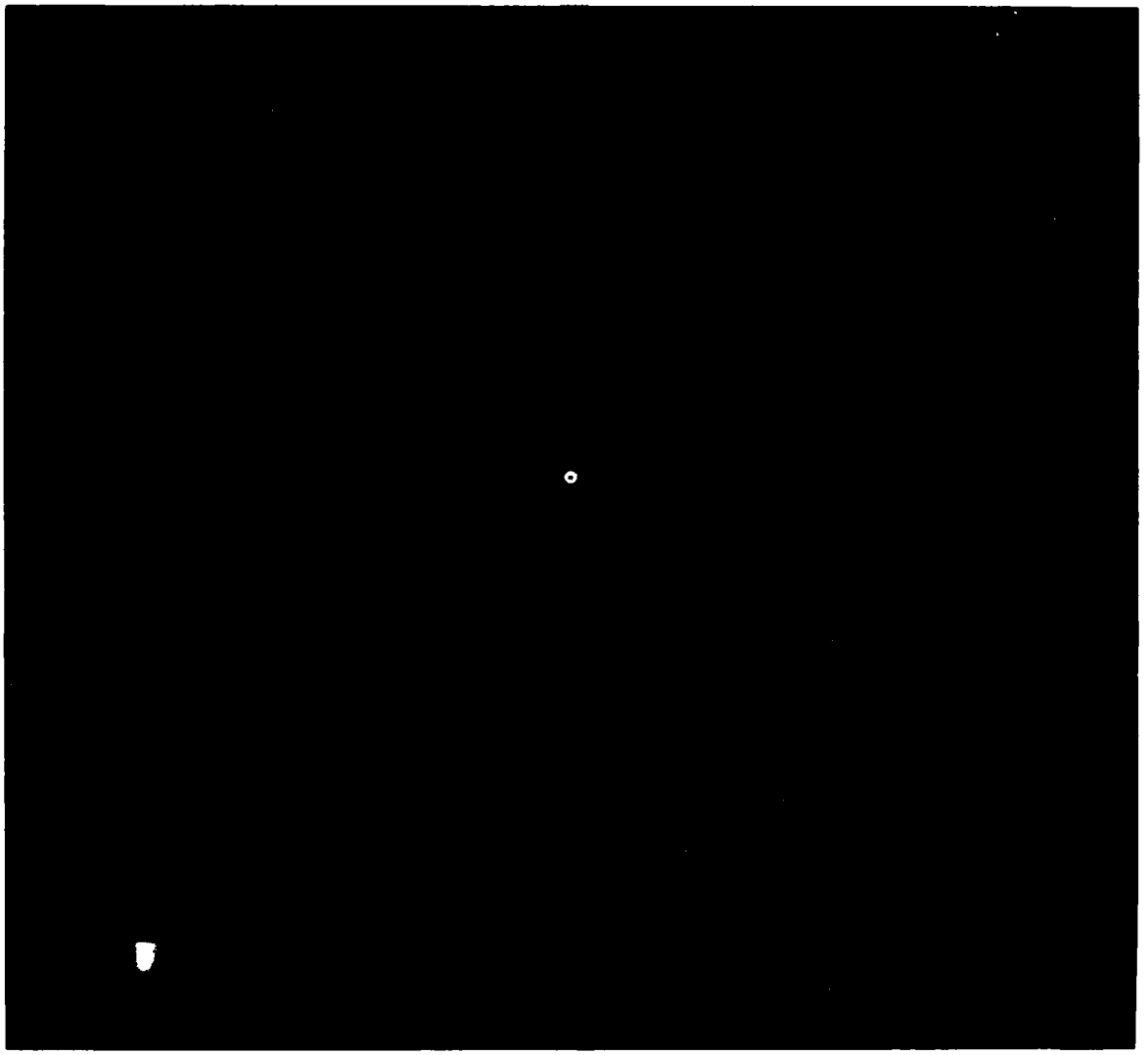

Figure 7. Point response function for the discrete element infilled aperture (finite bandpass and point elements, 15 element case). The scale has been adjusted to show detail in the sidelobes. This corresponds to PSF$_{1,2}$ in Fig. 4.

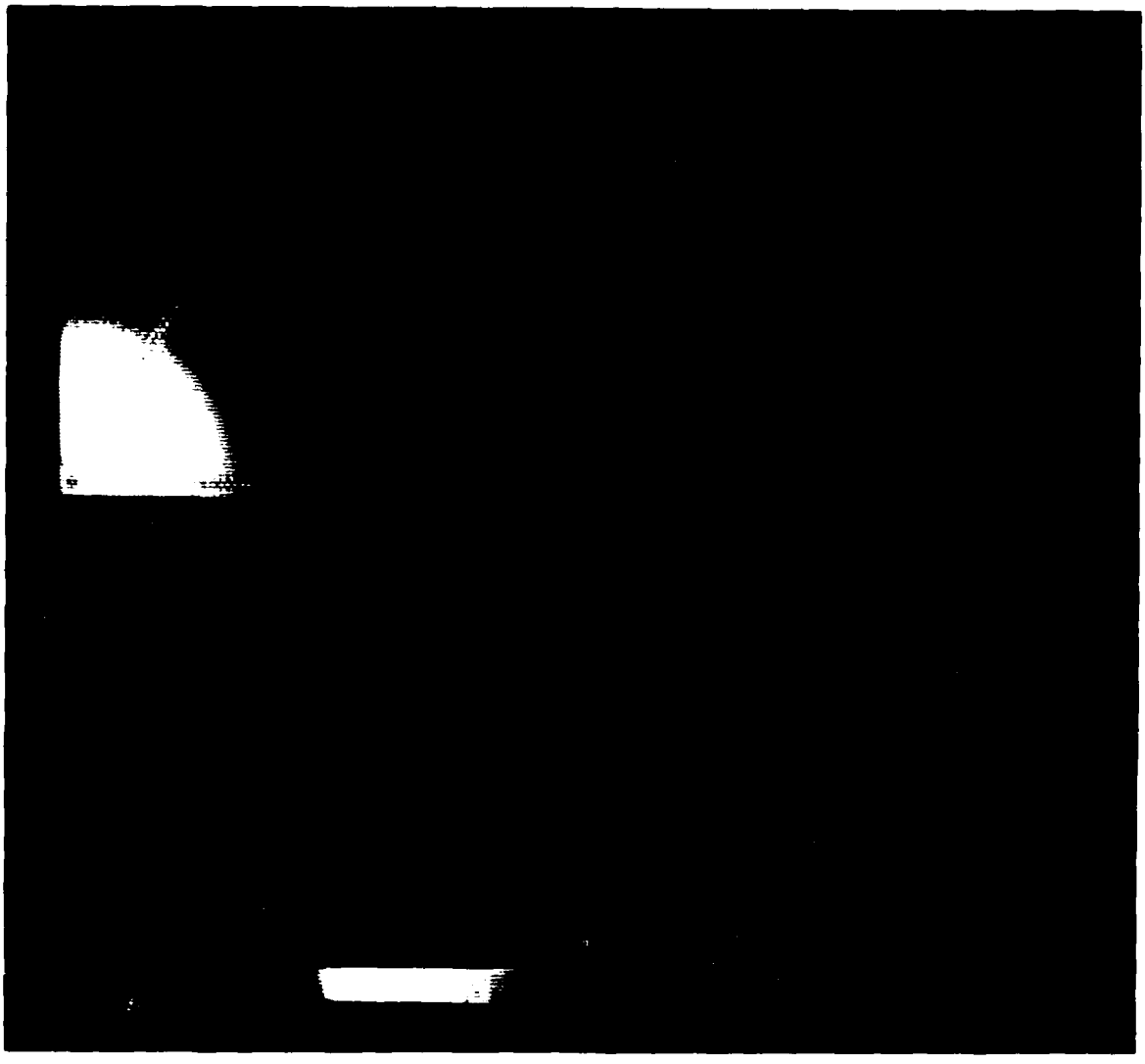

Figure 8. Point response functions for the four discrete-element unfilled apertures (finite bandpass and finite elements) considered in detail. Upper-left is for a three station interferometer; upper-right for a seven element array; lower-left for a 15-element array; and lower right for a 27-element array. Only one quadrant has been presented of each point response function for compactness. The scale is the same for each image, so that the improvement in the point response function as the number of stations increases can be seen. These maps correspond to PRF.MAP in Fig. 4.

(Page 20 Blank)

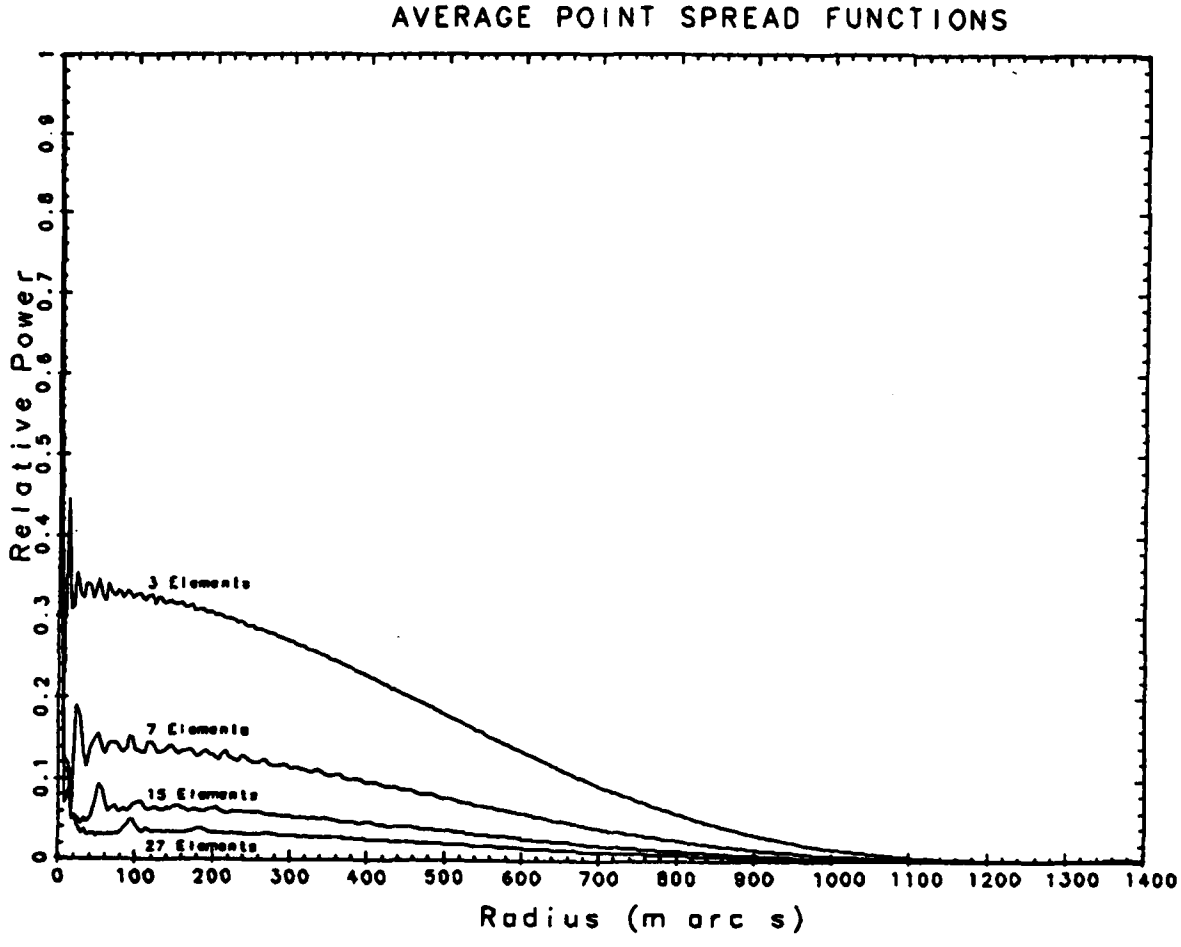

Figure 9. Point response functions for 3-, 7-, 15-, and 27-element unfilled apertures averaged in azimuth as a function of radial distance from the origin.

One approximation made in our calculations of point response functions was the assumption that the individual elements were small in comparison with the overall size of the array. In AIPS, to account for identical finite elements exactly would require adjusting the convolution function to be used for gridding the data into the UV plane so that the gridded data would be the autocorrelation (weighted UV coverage) of the individual array elements. This would be a minor correction in the analysis we did.

RESULTS

The point response functions in Fig. 8 are the principal result of this report. The images in Fig. 8 are the accurate two-dimensional representation of the point response functions for the finite-bandpass, finite-element, unfilled arrays which we studied using the analysis of the previous section. The point response functions have been shown using a color wedge which suppresses the central maximum (which appears only as a few pixels of red in the lower left of each image) in order to make the differences between the point response functions apparent. The six radial sidelobe arms in the 3-element case and the fourteen radial sidelobe arms in the 7-element case are remnants of incomplete sidelobe suppression by the delay function of the type shown in Fig. 6. As the number of elements increases, this delay sidelobe supression becomes more complete.

In comparison, the point response functions for the circularly-symmetric, monochromatic cases we considered are both simpler and much easier to calculate. The two dimensional point response functions shown in Fig. 8 are more complex, but are easily understood in terms of the circularly symmetric cases.

The sidelobes of the point response functions shown in Fig. 8 for the 3-, 7-, 15-, and 27-element unfilled apertures with finite bandpass and finite element size have two major components: (1) A pedestal caused by the response of the individual elements in the array, and (2) Oscillations about this pedestal due to the synthesized beam component. The peak level of the smooth pedestal component decreases as 1/N, as can be seen in Fig. 9 where the point response functions have been averaged in azimuth. The rms noise level of the synthesized beam component also decreases as 1/N. Thus the sidelobes decrease rapidly as the number of elements increases until approximately 7 to 15 elements are in the array. Larger numbers of elements then continue to improve the performance, but only at a slower rate; a specific desired imaging capability may lead to arrays of these dimensions. At the same time, the sampling in the U,V (Fourier transform) space is becoming more complete and the synthesized beam sidelobes are decreasing. By the time N is 7, the first sidelobe is 19% but the average oscillations about the 1/N pedestal level of 14% are at the 2% level. For the array geometries studied in this report, the larger number of elements also decreases the minimum spacing in the U,V plane, lowering the lowest spatial frequency sampled, and moving the first grating sidelobe (a circular ring for this geometry) further from the center.

The point response functions in Fig. 8 could be improved through image processing, with the degree of improvement depending on the field to be imaged as well as on the array characteristics. Because the array geometry, wavelength, and bandpass would be known, the point response function could be used to deconvolve the measured image and yield an accurate representation of the true image. A limitation is that the presently popular algorithms for deconvolution yield better (higher contrast) results as the sidelobes are lower, and as the measured signals fill a smaller percentage of the image pixels.

It is thus possible to specify the required number of elements for an array in two ways. First, the raw (no image-processing) contrast ratio required in the output image could be specified. Since the number of elements determines the sidelobe level more or less directly for this family of unfilled arrays, it is possible to invert the process and specify a required contrast ratio for the unprocessed image and yield the number of elements. For instance, in a satellite surveillance system where image processing in space is prohibited, a requirement of a 25:1 raw contrast specifies 25 elements. However, it should be emphasized that most applications do allow image processing, even if not with electronic digital computers, and such processing can improve the images significantly. This suggests the second method to specify the required number of elements: select the desired contrast ratio for a processed image. Since the contrast in a deconvolved, processed image depends not only on the array configuration but also on the complexity of the image and the signal-strength in the image, some broad characteristics for the field being imaged would need to be specified. Depending on the field being imaged, 10- to 50-fold increases in contrast ratio could be achieved. This sort of improvement is routinely achieved in images produced from radio interferometers.

CONCLUSIONS

This report demonstrates a new technique for modeling point response functions for complex interferometer systems taking into account both finite bandpass and finite element size. New interferometer systems can be fully evaluated with a few weeks of effort. While the analysis system is not trivial to use, it is straight forward as shown in Fig. 4.

In view of the limits to the overall size of the point response function imposed by the effects of broad bandwidth (see above), it is possible to choose between the two basic types of interferometers used in imaging. The first type, commonly used in radio-frequency imaging arrays such as the VLA, uses phase steering to map an image. The maximum image size is limited both by the UV coverage of the interferometer (the usual case) and the bandpass response of the array and receivers. With the narrow bandwidths available to radio-frequency detectors, this is a practical technique and allows the mapping of large fields with high resolution. The second type using delay steering is required where broad-band phase stable correlators are impractical to construct, such as at optical wavelengths. The advantage of the second method (where beams from the individual elements are combined coherently using mirrors and focused onto a detector array) is that large bandwidth is easily achieved along with a narrow point response function. The detectors for such an interferometer are directly measuring the convolution of the point response function with the true image; for many sorts of images reliable deconvolution (restoration) techniques exist, resulting in interferometer performance which equals that from a filled aperture.

The problem of restoring a complex image is expected to be worse for the case of a quasi-optical system viewing the earth than for the case of the radio images of celestial objects that radio astronomers typically restore. However, many of the standard radio astronomy image processing techniques are directly applicable. It is important to note there are proven techniques to deconvolve images to reduce the sidelobe levels below those presented in Fig. 9. The exact effects of sidelobe levels and the extent to which they could be removed will depend on the exact constraints and design parameters for a real system as well as on the characteristics of the field under observation.

As a demonstration of the discrete analysis system, a spaceborne earth monitoring optical (350-650 nm) interferometer system was modeled to determine the number of elements needed to provide satisfactory performance. We fixed the maximum baseline length at 10 m, the size of each element at 10 cm, the geometry to evenly spaced elements on a ring, and varied the number of elements between 3 and 99.

We find the sidelobe level for a monochromatic system varies as the reciprocal of the number of elements over the range of interest in this study. This establishes an upper limit for any realistic system, because the finite element size reduces sidelobes as was shown above.

We find the realistic bandpasses of interest limit the sidelobes to such a level that they are of little concern for arrays with more than a few elements.

We find that the difference between an addition correlator and a multiplication correlator is not significant in either the difficulty of analysis or the performance of a large number of elements.

REFERENCES

1. Thompson, A. R., Clark, B. G. , Wade, C. M. , and Napier, P. J., "The Very Large Array", Ap. J. Suppl., vol 44, p. 151, October 1980.
2. National Radio Astronomy Observatory, "The Very Long Baseline Interferometer Array Design Study", NRAO (Green Bank, WV), February 1981.
3. Born, Max and Wolf, Emil, "Principles of Optics", 3rd Edition, Pergamon Press (New York) 1965, pp. 256-259.
4. Born, Max and Wolf, Emil, op. cit., pp. 392-398.
5. Pearson, T. J., "Caltech VLBI Reduction Programs", private communication, Caltech, mailstop 102-24, Pasadena, CA 91125.
6. National Radio Astronomy Observatory, "The AIPS Computer Program Package", NRAO, Charlottesville, VA.
7. "IDL User's Guide", by Research Systems, Inc., (Denver, CO), 1982.

APPENDIX A

BANDWIDTH EFFECTS

INTRODUCTION

The following discussion closely follows the development of Thompson (1982) which was for the particular case of the VLA for radio astronomy. First the two element interferometer with rectangular bandpass is considered. Non rectangular bandpasses only make the mathematics harder to solve in closed form, but are not intrinsically difficult. The solution for two elements is a sin(x)/x function. In going over to the array case, a superposition of solutions with the correct weighting is required. In practice it is appropriate to restart the analysis. However, this approach requires the fractional bandpass to be small ($\sim$ 5%) in order for the mathematics to reduce to simple form. For wide bandpasses, the mathematics probably gets more involved, and a computer summation is the expediant solution. The paper of Thompson paraphrased in part here sets the framework for more detailed analysis at a later time.

BANDWIDTH EFFECT FOR 2 ELEMENT INTERFEROMETER

The part of the interferometer in which the signals are combined is the correlator, which is basically a voltage multiplier and a time averager. Its output is the real part of V' and is related to the input voltage waveforms V_1 and V_2 by:

$$R_e(V') = \langle V_1^*(t)\ V_2\ (t+\tau)\rangle \qquad \text{(A-1)}$$

where the angular brackets represent a time average and we have taken the complex conjugate of the first waveform.

Let $I(\vec{s},\nu)$ represent the brightness (intensity) of the target in the direction of unit vector $\vec{s}$ at a frequency ν. The signal power received in a bandwidth $d\nu$ from the source $d\Omega$ is $A(\vec{s})\,I(\vec{s})\,d\Omega\,d\nu$, where $A(\vec{s})$ is the effective collecting area in direction $\vec{s}$ which is assumed to be the same for each interferometer element.

If the inputs to the correlator are represented by the complex analytic signals the received power is equal to the square of the modulus, and thus:

$$|v_1|^2 = |v_2|^2 = |v_1 v_2| = A(\vec{s})I(\vec{s})d\Omega d\nu. \qquad \text{(A-2)}$$

In the case where the elements are not identical, A is replaced by the product of the complex voltage responses of the elements. The arguments of v_1 and v_2 are given by:

$$\begin{aligned} \arg[v_1] &= 2\pi\nu t \\ \arg[v_2] &= 2\pi\nu(t+\tau) \end{aligned} \qquad \text{(A-3)}$$

where τ is the difference between the geometrical and instrumental delays in Fig. A-1. If $\vec{B}$ is the baseline vector for the two antennas,

$$\tau = \tau_g - \tau_i = \vec{B}\cdot\vec{s}\ c^{-1} - \tau_i . \qquad \text{(A-4)}$$

Then from (A-1) with appropriate integration we obtain the total response:

$$V'(\vec{s},\tau_i)d\nu = \int_{-\infty}^{\infty} \int_S A(\vec{s},\nu) e^{i2\pi\nu(\vec{B}\cdot\vec{s}c^{-1}-\tau)} d\Omega d\nu \qquad \text{(A-5)}$$

where S indicates that the integral with respect to Ω is taken over the surface of the hemisphere. If we take the Fourier transform of V' with respect to τ_i we obtain:

$$V(\vec{B},\nu) = \int_{-\infty}^{\infty} V'(\vec{B},\tau_i) e^{i2\pi\nu\tau_i}\, d\tau$$

$$V(\vec{B},\nu) = \frac{1}{\Delta\nu} \int_{\nu_o-\Delta\nu/2}^{\nu_o+\Delta\nu/2} \int_S A(\vec{s},\nu) I(\vec{s},\nu) e^{i2\pi\nu\vec{B}\cdot\vec{s}/c}\ d\Omega\ d\nu \qquad \text{(A-6)}$$

and the integral over frequency depends upon the bandpass*. Often over the bandwidth $\Delta\nu$ the quantities V, A and I can be assumed constant and we can write them as functions of $\vec{B}$ or $\vec{s}$ only, with the understanding that they refer to a center frequency ν_o. Thus (A-6) simplifies to

$$V(\vec{B}) = \int_S A(\vec{s}) I(\vec{s}) e^{i2\pi\nu_o\vec{B}\cdot\vec{s}/c}\ d\Omega \qquad \text{(A-7)}$$

This is the monochromatic result that is usually used for narrow band-passes.

If we assume $A(\vec{s},\nu)$ is a rectangular bandpass from $\nu_o-\Delta\nu/2$ to $\nu_o+\Delta\nu/2$, then the Fourier transform of a rectangle is a sin(x)/x function yielding

$$V(\vec{B}) = \int_S \frac{\sin[\pi\Delta\nu\vec{B}\cdot(\vec{s}-\vec{s}_o)/c]}{\pi\Delta\nu\vec{B}\cdot(\vec{s}-\vec{s}_o)/c} A(\vec{s}) I(\vec{s}) e^{i2\pi\nu_o\vec{B}(\vec{s}-\vec{s}_o)/c}\ d\Omega \qquad \text{(A-8)}$$

Here we have assumed that the passband is rectangular with center frequency ν_o and width $\Delta\nu$, and $\vec{s}_o$ is the direction for which the instrumental delay is adjusted to compensate for the geometrical delay. In the simple interferometer in Fig. A1 the direction $\vec{s}_o$ is indicated by the angle θ_o measured with respect to a plane normal to the baseline. Since $\vec{B}\cdot(\vec{s}-\vec{s}_o) \approx B(\theta-\theta_o)\cos\theta_o$ we see from (A-8) that for a point source at position θ_o the effect of the finite bandwidth is to multiply the response by the sinc function

$$\frac{\sin[\pi\Delta\nu b(\theta-\theta_o)\cos\theta_o c^{-1}]}{\pi\Delta\nu B(\theta-\theta_o)\cos\theta_o c^{-1}} \qquad \text{(A-9)}$$

*The sign convention for the exponential, here positive for transforming from I to V, varies between authors but is inconsequential in these general discussions.

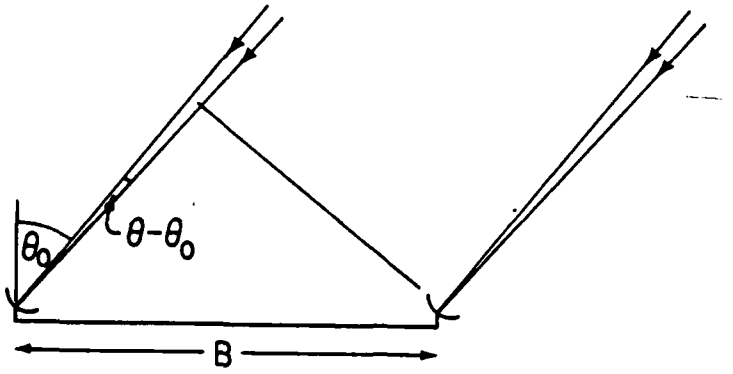

Figure A1. Angles of the incident radiation.

As a function of θ, the output is a product of the fringe pattern and the sinc function which modulates the fringes. The latter term can be regarded as resulting from the decorrelation of the signals produced by the inequality of the time delays for directions other than θ_o. From the Weiner-Khinchine theorem the autocorrelation function of the signals is the Fourier transform of the power spectrum, and hence the rectangular passband gives rise to the sinc function term. This term limits the response in a manner that has some similarity to an antenna beam, and the result is sometimes referred to as the "delay beam". It is an example of what has been more generally referred to as space-frequency synthesis. Swenson and Mathur (1969) have shown that there is an exact correspondence between frequency and antenna spacing in determining the spatial frequency response of a pair of radio antennas. Some radio arrays have been constructed to make particular use of this principle; see, for example, Douglas et al. (1973). It is also of particular importance in very long baseline interferometry (Robertson et al. 1982). Note however that the envelope function falls to half amplitude at $(\theta-\theta_o) = 0.6c(B \cos\theta_o \Delta\nu)^{-1}$, i.e. the delay 'beamwidth' depends upon the projected antenna spacing $B\cos\theta_o$. For an array with numerous element spacings the beamwidth concept is inappropriate and it is better to examine the problem as in the following section.

BANDWIDTH EFFECT FOR AN ARRAY

The relationship between the measured visibility, V(u,v), and the distribution of intensity of brightness, I(x,y) can, with certain assumptions, be written as

$$V(u,v)S(u,v)w(u,v) \rightleftharpoons I(x,y) * * b(x,y) \qquad \text{(A-10)}$$

where

- S(u,v) = sampling function that represents the distribution of the data points in the (u,v) plane.
- w(u,v) = weighting function of the data including any applied tapering. S(u,v)w(u,v) is the optical modulation transfer function.
- b(x,y) = synthesized beam.
- I(x,y) = brightness distribution as modified by the beams of the individual elements.
- $\rightleftharpoons$ = denotes Fourier transformation.
- * * = denotes two-dimensional convolution.

The synthesized beam is defined as the Fourier transform of $S(u,v)w(u,v)$, and it is equal to the response to a point source at the (x,y) origin. (To be precise, the response to a point source is often defined as the mirror image of the beam, i.e. $b(-x,-y)$. In this case $S(u,v)w(u,v)$ is entirely real so $b(x,y)$ is symmetrical and the distinction can be ignored. The effects discussed here that result in distortion of the response to a point source are usually zero at the (x,y) origin, which is why we have stated that $b(x,y)$ is pthe response to a point source at that position. If $b(x,y)$ varies over the (x,y) plane equation (A-10) does not, of course, hold. In using (A-10) we therefore assume that the various distorting effects to be described are negligible; in particular we shall apply (A-10) only to an incremental frequency bandwidth $d\nu$ centered at frequency ν within the receiving passband. Let (u_ν, v_ν) be the spatial frequency coordinates that correspond to frequency ν. In reducing the visibility data in the usual way for continuum observations we treat the data derived from the full receiving passband as though all of the signal was at the center frequency ν_o. Thus, since u and v are measured in wavelengths, the assigned values for frequency ν are

$$\left(\frac{\nu_o u_\nu}{\nu}, \frac{\nu_o v_\nu}{\nu}\right)$$

wavelengths. For the frequency increment $d\nu$ equation (A-10) becomes

$$V\left(\frac{\nu_o u_\nu}{\nu}, \frac{\nu_o v_\nu}{\nu}\right) S(u,v)w(u,v) \rightleftharpoons \left(\frac{\nu}{\nu_o}\right)^2 I\left(\frac{\nu_o x}{\nu}, \frac{\nu_o y}{\nu}\right) * * b(x,y) \qquad \text{(A-11)}$$

Here we have used the similarity theorem of Bracewell (1965) which, in one dimension, can be stated as follows:

$$\text{if } g(u) \rightleftharpoons f(x), \text{ then } g(au) \rightleftharpoons \frac{1}{|a|} f\left(\frac{x}{a}\right).$$

Note that in (A-11) it has been assumed that V and I do not vary appreciably with ν over the receiving passband. Because we assign values of u and v that do not vary with ν, it follows that S, w and b do not vary with ν. However, this assignment introduces a scaling error ν/ν_o in the brightness coordinates. The measured distribution is obtained by averaging the right-hand side of (A-11) over the receiving passband:

$$I_1(x,y) = \left[\frac{\int_o^\infty \left(\frac{\nu}{\nu_o}\right)^2 P(\nu) I\left(\frac{x\nu}{\nu_o}, \frac{y\nu}{\nu_o}\right) d\nu}{\int_o^\infty P(\nu) d\nu}\right] * * b(x,y) \qquad \text{(A-12)}$$

where $P(\nu)$ is the power response of the receiving system. In deriving (A-12) we have integrated over bandwidth after Fourier transformation to the (x,y) domain, but the end result is identical to integration over bandwidth in the (u,v) domain which is implicit in the usual data-processing

The variation of the scale of x and y with ν in (A-12) is clearly a radial effect, and averaging over the bandwidth therefore results in a radial broadening or smearing of the detail. We see from (A-12) that the measured brightness distribution is a modification of the true brightness in which the radial smearing is first applied and then the resulting distribution is

convolved with the synthesized beam. The extent of the smearing increases in proportion to the distance from the (x,y) origin. However, ringlobe responses of the synthesized beam are smeared to the same extent as the main beam response, even if they fall near the origin, as illustrated in Fig. A2. Note

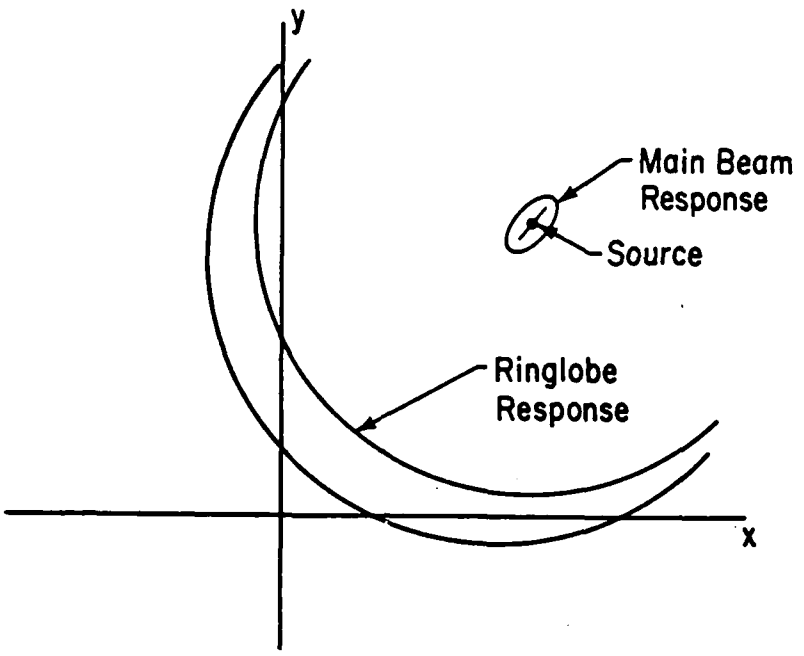

Figure A2: Response to a point source displaced from the (x,y) origin when the synthesized beam contains a ringlobe. The main beam and all sidelobes are broadened in the radial direction by convolution with the radially-smeared point source.

that the synthesized beam, as we have defined in above, does not vary over the map. However, the response to a point source does vary, because of the radial smearing, and this response is often regarded as defining the beam for practical purposes. Statements about the behavior of the 'beam' can therefore lead to confusion if the meaning of the term is not made clear.

The radial smearing reduces the amplitude of the response to a source by an amount that depends upon the source position and the radial width of the response. As an example we can calculate the reduction for a point source for a case where the synthesized beam is represented by a Gaussian distribution. Figure A3 shows a radial section through the response to such a source at a

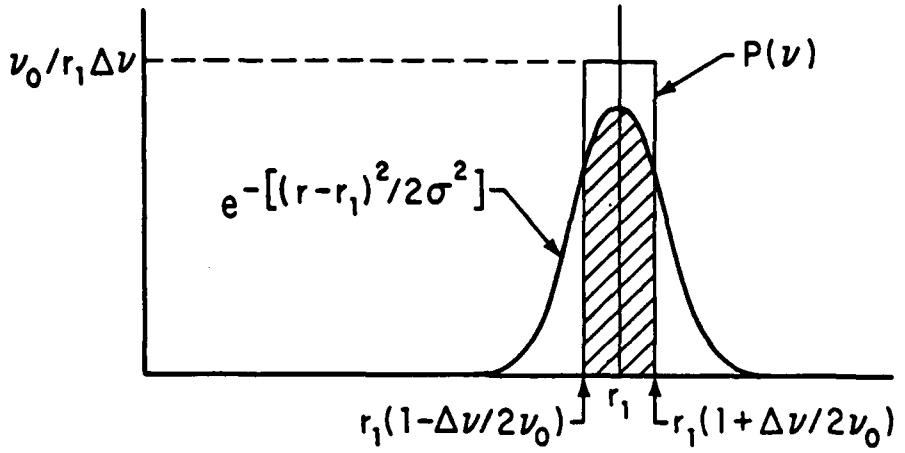

Figure A3: Radial section through point source at r_1 which is spread into a rectangular distribution by the finite receiving bandwidth. The Gaussian function represents the syntehsized beam.

distance r_1 from the origin. We shall represent the bandpass function $P(\nu)$ by a rectangular function of width $\Delta\nu$, and ignore the factor $(\nu/\nu_o)^2$ in the numerator of (A-12) since it is unlikely that it differs from unity by more than 5%. Then the broadened source is represented by the rectangle in Fig. A3, and the peak response by the area under the product of the two function. The ratio, R_B, of the peak response relative to that when $\Delta\nu$ tends to zero is

$$R_B = \frac{\nu_o}{r_1\Delta\nu}\int_{r_1(1-\Delta\nu/2\nu_o)}^{r_1(1+\Delta\nu/2\nu_o)} e^{-(r-r_1)^2/2\sigma^2}\,dr = \frac{\sqrt{2\pi}\,\sigma\,\nu_o}{r_1\Delta\nu}\,\mathrm{erf}\left(\frac{r_1\Delta\nu}{2\sqrt{2}\,\sigma\,\nu_o}\right) \qquad \text{(A-13)}$$

where erf ( ) is the normal error function. The half-power width of the synthesized beam, θ_b, is 2.35σ, and in terms of θ_b

$$R_B = 1.064\left(\frac{\theta_b\nu_o}{r_1\Delta\nu}\right)\mathrm{erf}\left(\frac{0.832\,r_1\Delta\nu}{\theta_b\,\nu_o}\right) \qquad \text{(A-14)}$$

A graph of this function is shown in Fig. A4. The response is reduced by a factor 1/2 when $(r_1\Delta\nu/\theta_b\nu_o) = 2.1$, and for $r_1\Delta\nu \gg \theta_b\nu_o$, the response decreases approximately as $(r_1\Delta\nu)^{-1}$.

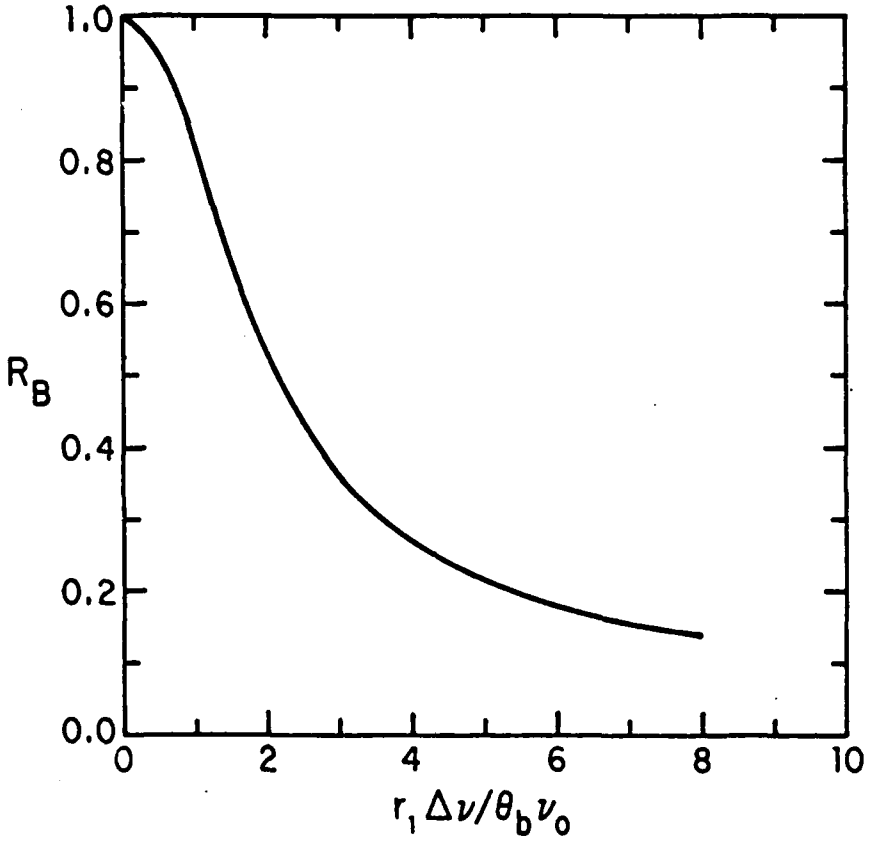

Figure A4: Decrease in the response to a point source with increasing distance from the field center, from equation (A-14).

Although the peak response to a point source i.e. the apparent brightness in the map is decreased by the radial smearing, the response is also broadened and it is easy to see that the integrated flux density remains unchanged. The broadening of the response for a point source can be calculated by convolving the bandpass function with the synthesized beam profile as indicated by equation (A-12).

References for Appendix A

Swenson, G. W. Jr., and Mathur, N. C. (1969), Radio Science, 4, 69-71.

Douglas et al. (1973) Astron. J., 78, 1-17.

Thompson, A. R. (1982), "The Effects of Bandwidth and Similar Parameters", Chapter 5 of Synthesis Mapping, Thompson and D'Addario, eds. NRAO (Green Bank, West Virginia).

Bracewell, R. N. (1965) The Fourier Transform and its Application, McGraw-Hill, New York.

Robertson, D. S., and Carter, W. E. (1982) "Operation of the National Geodetic Survey POLARIS Network", in Proceedings of Symposium No. 5: Geodetic Applications of Radio Interferometry, Inter. Assoc. of Geodesy, NOAA, 63-70.

APPENDIX B

PROGRAM SOURCE CODE and DATA FILES

I. Files used in running FAKE:

The following DCL command procedure runs the Caltech VLBI program FAKE for the case of 15 elements whose locations are specified in the STATIONS.DAT file. The start time has been selected so as to give one baseline exactly north-south, for compatibility with later programs.

FAKE.COM

```
! Assignment to specify station position file:
$ ASSIGN STATIONS.DAT STATIONS
$
$ FAKE                  ! Start the program

OUTPUT='15STA.DAT'      ! Name of output data file
MODEL='POINT.MOD'       ! Name of input model file

YEAR=1983               ! Year, date, start and stop selected so
DAY 356                 !   as to give a single integration period
START 23:56:00          !   for the data set with the correct
STOP 00:03:00           !   orientation
INTEG 600               !

FREQ 27037              ! This frequency, in combination with
                        ! the STATIONS.DAT file gives an array of
                        ! diameter 20 million G

RA 00:00:01             ! Source position
DEC 89:50:00            !

STATIONS '15N1', '15N2', '15N3', '15N4', '15N5',
         '15N6', '15N7', '15N8', '15N9', '15N10',
         '15N11','15N12','15N13','15N14','15N15'

PHASES 0.   ERRADD 0.000001  ERRMULT 0.0       /
```

Data files used by FAKE

The following is an example of the STATIONS.DAT file used by FAKE. Note that in its current incarnation, FAKE requires this to be in fixed format.

STATIONS.DAT

15N1	0.	89.0	24.0	80.0
15N2	0.	89.0	48.0	80.0
15N3	0.	89.0	72.0	80.0
15N4	0.	89.0	96.0	80.0
15N5	0.	89.0	120.0	80.0
15N6	0.	89.0	144.0	80.0
15N7	0.	89.0	168.0	80.0
15N8	0.	89.0	192.0	80.0
15N9	0.	89.0	216.0	80.0
15N10	0.	89.0	240.0	80.0
15N11	0.	89.0	264.0	80.0
15N12	0.	89.0	288.0	80.0
15N13	0.	89.0	312.0	80.0
15N14	0.	89.0	336.0	80.0
15N15	0.	89.0	360.0	80.0

The following is an example of the fake source file POINT.MOD

POINT.MOD

```
! Sample fake data file
!
! The following is a 1-Jy point source.
! Flux    Radius    Theta    Axis   Ratio    Phi    Type
   1        0         0       0       0       0       1
```

II. Bandpass program

```
C                              Program BAND
C
C       BAND computes the bandwidth-dependent beam for an interferometer
C       by summing the appropriate sinc functions into an array.  It
C       assumes the elements are evenly spaced on a ring;  only odd numbers
C       of elements up to MAXS elements are allowed.
C
C       When linking this program, both the Caltech VLBI object library
C       and the Caltech public object library need to be accessed.
C
C       Parameters:
        CHARACTER*(*) VERSION
        CHARACTER*12 ELAPSE
        INTEGER*4 INC,OUTC,OUTDAT,MAXS,MAXB,MAXP,NPARS
        REAL*8 PI,VELC
        PARAMETER (VERSION='1.0 - 1983 January 28')
        PARAMETER (INC=5,OUTC=6,OUTDAT=10)
        PARAMETER (MAXS=99)      ! maximum number of stations
        PARAMETER (MAXB=(MAXS-1)*MAXS/2)
        PARAMETER (MAXP=MAXB)    ! maximum number of u,v-points
        PARAMETER (NPARS=14)     ! input parameters
        PARAMETER (PI=3.141592653589793D0)      ! pi
        PARAMETER (VELC=2.997925D8)             ! speed of light
C
        REAL*8  PARS(NPARS),VALS(NPARS),ENDMRK
        REAL*4  POSANG(MAXS),BUFFER(512,512)
        INTEGER*2 IARRAY(512),IX,IY
        CHARACTER*64 OUTDSN
        EQUIVALENCE (OUTDSN,VALS(7))
        CHARACTER TODAY*9,NOW*8
        DATA      PARS/ 'NSTA', 'DIAMETER', 'FOV', 'LMIN',
     1                  'LMAX', 'PIXELS', 'OUTFILE', 7*'       ' /
        DATA      VALS/ 3D0,   10D0,    2048D0, 3500D0,
     1                  6500D0, 512D0, 8*'        ' /
        DATA      ENDMRK/ '/' /
C
C               Introduction
C
        CALL DATE(TODAY)
        CALL TIME(NOW)
        WRITE(OUTC,1001) VERSION
C
C               Control parameters
C
   10   WRITE(OUTC,1001) ' Parameters (type HELP for details):'
        MODE = 1
        IF (ISTERM('SYS$INPUT')) MODE = 2
        CALL KEYIN(PARS,VALS,NPARS,ENDMRK,MODE,INC,OUTC)
C
C               Check parameter values
C
```

```
      IF (VALS(1) .GT. MAXS .AND.
     +   INT(VALS(1)-1D0)/2 .NE. INT(VALS(1)) .AND.
     +   VALS(1) .NE. 2 .AND. VALS(1) .NE. 4) THEN
          WRITE (OUTC,1000)' Illegal number of stations.  Try again',
     +   ', please.'
          GO TO 10
        ELSEIF (VALS(6) .NE. 512 .AND.
     +   VALS(6) .NE. 256 .AND. VALS(6) .NE. 128 .AND.
     +   VALS(6) .NE. 64 .AND. VALS(6) .NE. 32) THEN
          WRITE (OUTC,1000)' Illegal number of pixels.  Try again,',
     +   ' please.'
          GO TO 10
        ELSE
C         Attempt to open output file
          IF (OUTDSN .EQ. ' ') GO TO 20
          CLOSE (UNIT=10)
          IMSIZE = VALS(6)
          OPEN(UNIT=OUTDAT,NAME=OUTDSN,STATUS='NEW',
     1    FORM='UNFORMATTED',RECORDTYPE='FIXED',RECL=IMSIZE/2,ERR=20)
          INQUIRE(UNIT=OUTDAT,NAME=OUTDSN)
          GOTO 30
   20     WRITE (OUTC,1000)' Unable to open output file.  Please try',
     +   ' again.'
          GO TO 10
   30     CONTINUE
        ENDIF
        NSTA = VALS(1)
C
C       Write out input parameters with units
        WRITE (OUTC,1002) NSTA,(VALS(I),I=2,5),IMSIZE,
     +  OUTDSN(1:LEN1(OUTDSN))
C
C       Calculate array, one position angle and baseline at a time
        IF (NSTA .EQ. 2) THEN
          POSANG(1) = 90
        ELSE
          DO I=1,(NSTA-1)/2
            POSANG(I) = I*(180./NSTA) - 90.
          ENDDO
        ENDIF
        NBASE = NSTA*(NSTA-1)/2
        NLENGTH = (NSTA-1)/2
C
C       Begin array calculations here
        DELAY = 1D10 * PI * ABS(1/VALS(4) - 1/VALS(5))
        FOV = (VALS(3) * PI) / (180. * 3600. * 1000)
        CALL RCLOCK(ELAPSE,CPU)
        WRITE (6,1000) ' Ready to start long calculation.'
        WRITE (6,1003) ELAPSE,CPU
C
```

```
      DO IL = 1,NLENGTH
        BSLINE = VALS(2)*COS((IL-0.5)*PI/NSTA)
        DO IB = 1,(NSTA-1)/2
C         Calculate 1st half of array:
          CALL ARRAY(DELAY,BSLINE,FOV,POSANG(IB),IMSIZE,BUFFER)
        ENDDO
      ENDDO
C
      CALL RCLOCK(ELAPSE,CPU)
      WRITE (6,1000) ' Long calculation finished.'
      WRITE (6,1003) ELAPSE,CPU
C
C     Now, load up upper half of array
      DO IX = 1,IMSIZE
        DO IY = 2,(IMSIZE/2)+1
          BUFFER(IMSIZE-IX,IMSIZE+2-IY) = BUFFER(IX,IY)
        ENDDO
      ENDDO
C
C     Multiply this first half of array by 2 for normalization reasons
      DO IY = 1,IMSIZE
        DO IX = 1,IMSIZE
          BUFFER(IX,IY) = BUFFER(IX,IY) + BUFFER(IX,IY)
        ENDDO
      ENDDO
C
C     Add in the pa=90 and pa=0 contribution (if any)
      DO IL = 1,NLENGTH
        BSLINE = VALS(2)*COS((IL-0.5)*PI/NSTA)
        CALL ARRAY(DELAY,BSLINE,FOV,90.,IMSIZE,BUFFER)
        IF (NSTA .EQ. (NSTA/2)*2) THEN
C         Number of stations is even
          CALL ARRAY(DELAY,BSLINE,FOV,0.,IMSIZE,BUFFER)
        ENDIF
      ENDDO
C
C     Now, flip array over and add into final result, then
C     write out array into file after normalizing
      PEAK = 2 * NBASE
      DO IY = 1,IMSIZE
        DO IX = 1,IMSIZE-1
          IARRAY(IX) = 32767 *
     +                 (BUFFER(IX,IY)+BUFFER(IMSIZE-IX,IY)) / PEAK
        ENDDO
        IARRAY(IMSIZE) = 0 ! Since flip was not valid for that column
        WRITE (10) (IARRAY(IX), IX=1,IMSIZE)
      ENDDO
      CLOSE (UNIT=10)
      STOP
C
C
 1000 FORMAT(A)
 1001 FORMAT(' BAND calculates the delay beam for simple arrays',
     +       /' (Version ',A,')'/)
```

```
 1002   FORMAT (' Input parameters:'/
     +  ' ',I8,2X,'=  number of stations.'/
     +  ' ',F8.2,2X,'=  array diameter in meters.'/
     +  ' ',F8.2,2X,'=  field of view, in mas.'/
     +  ' ',F8.1,2X,'=  lower wavelength, angstroms.'/
     +  ' ',F8.1,2X,'=  upper wavelength, angstroms.'/
     +  ' ',I8,2X,'=  output image size.'//
     +  ' Output to file ',A)
 1003   FORMAT (' Elapsed time: ',A,'  CPU:',F15.3)
C
       END



       SUBROUTINE ARRAY(DELAY,BSLINE,FOV,POSANG,IMSIZE,BUFFER)
C
C            Calculate array:  Delay=pi* d nu * / c, in meters
C                              bsline=baseline in meters
C                              fov=field of view, in radians
C                              imsize=array size, in pixels
       REAL*8 PI
       PARAMETER (PI=3.141592653589793D0)      ! pi
       REAL*4 ROW(512),COLUMN(512),BUFFER(512,512)
       INTEGER*2 IX,IY,ICX,ICY
C
C      Center for AIPS
       ICX = IMSIZE/2
       ICY = ICX + 1
       RPOSANG = POSANG*PI/180.
       XUNIT = DELAY * BSLINE * FOV / IMSIZE
C
C
C      Calculate array, with special cases for 0 and 90 degrees
       IF (POSANG .EQ. 90.) THEN
         DO IY=1,IMSIZE
C          First, calculate a column in the array (x=1)
           X = XUNIT * RADIUS * ABS(ICY - IY)
           IF (X .EQ. 0.) THEN
             SINCX = 1
           ELSE
             SINCX = SIN(X) / X
           ENDIF
           COLUMN(IY) = SINCX
         ENDDO
         DO IY=1,IMSIZE
           DO IX=1,IMSIZE
             BUFFER(IX,IY) = BUFFER(IX,IY) + COLUMN(IY)
           ENDDO
         ENDDO
       ELSEIF (POSANG .EQ. 0.) THEN
         DO IX = 1,IMSIZE
C          First, calculate first ROW in array (y=1)
           X = XUNIT * RADIUS * ABS(ICX - IX)
```

```
            IF (X .EQ. 0.) THEN
              SINCX = 1
            ELSE
              SINCX = SIN(X) / X
            ENDIF
            ROW(IX) = SINCX
          ENDDO
          DO IY=1,IMSIZE
            DO IX=1,IMSIZE
              BUFFER(IX,IY) = BUFFER(IX,IY) + ROW(IX)
            ENDDO
          ENDDO
        ELSE
C
C         Calculate lower half of array
          DO IX = 1,IMSIZE
C           First, calculate first row in array (y=1)
            IDX = IX-ICX
            IDY = ICY-1
            RADIUS = SQRT(FLOAT(IDX**2 + IDY**2))
            ANGLE  = RPOSANG - ATAN2(FLOAT(IDX),FLOAT(IDY))
            X = ABS(SIN(ANGLE) * XUNIT * RADIUS)
            IF (X .EQ. 0.) THEN
              SINCX = 1
            ELSE
              SINCX = SIN(X) / X
            ENDIF
            BUFFER(IX,1) = BUFFER(IX,1) + SINCX
C
            DO IY = 2,ICY-1
              IDY = IY-ICY
              RADIUS = SQRT(FLOAT(IDX**2 + IDY**2))
              ANGLE  = RPOSANG - ATAN2(FLOAT(IDX),FLOAT(IDY))
              X = ABS(SIN(ANGLE) * XUNIT * RADIUS)
              IF (X .EQ. 0.) THEN
                SINCX = 1
              ELSE
                SINCX = SIN(X) / X
              ENDIF
              BUFFER(IX,IY) = BUFFER(IX,IY) + SINCX
            ENDDO
          ENDDO
C
C
          DO IX=1,ICX-1
            RADIUS=ICX-IX
            ANGLE = RPOSANG - PI/2.
            X = ABS(SIN(ANGLE) * XUNIT * RADIUS)
            IF (X .EQ. 0.) THEN
              SINCX = 1
            ELSE
              SINCX = SIN(X) / X
            ENDIF
            BUFFER(IX,ICY) = BUFFER(IX,ICY) + SINCX
```

```
            BUFFER(IMSIZE-IX,ICY) = BUFFER(IMSIZE-IX,ICY) + SINCX
          ENDDO
C
          BUFFER(ICX,ICY) = BUFFER(ICX,ICY) + 1.
        ENDIF
C
        RETURN
        END
```

III. Program to find radial point response function profiles.

```
C       Program POWER
C
C       This program finds the power for a 512 on a side
C       AIPS map, with the output in a 1-d array with average power as
C       a fn of radius from 256,257 in the output file.  The output file
C       is in LISTING format so that it may be printed, etc.
C
        CHARACTER*64 OUTDSN,INDSN
        PARAMETER IMSIZE=512
        REAL*4 POWER(IMSIZE)
        INTEGER*2 INDATA(IMSIZE,IMSIZE),MIN,MAX,IX,IY,IREC,IBIN,
     +  IWEIGHT(IMSIZE)
C
C       Attempt to open files
   10   WRITE (6,1000) '$Filename of AIPS map: '
        READ  (5,1000,END=99,ERR=10) INDSN
        CLOSE (UNIT=10)
        OPEN(UNIT=10,NAME=INDSN,STATUS='OLD',READONLY,
     1  FORM='UNFORMATTED',RECORDTYPE='FIXED',RECL=128)
        INQUIRE(UNIT=10,NAME=INDSN)
        GO TO 30
   20   WRITE (OUTC,1000)' Unable to open input file. '
        GO TO 10
   30   CONTINUE
C
C       Get output file
   40   WRITE (6,1000) '$Filename of output file: '
        READ  (5,1000,END=99,ERR=40) OUTDSN
        CLOSE (UNIT=11)
        OPEN(UNIT=11,NAME=OUTDSN,STATUS='NEW',
     1  FORM='FORMATTED',CARRIAGECONTROL='LIST',ERR=50)
        INQUIRE(UNIT=11,NAME=OUTDSN)
        GO TO 60
   50   WRITE (OUTC,1000)' Unable to open output file. '
        GO TO 40
   60   CONTINUE
C
        WRITE (6,1001)'0The input file is ',INDSN(1:LEN1(INDSN))
        WRITE (6,1001)'0The output file is ',OUTDSN(1:LEN1(OUTDSN))
C
C       READ IN DATA
        DO IY = 1,IMSIZE
          DO IREC=1,IMSIZE/256
            READ (10) (INDATA(IX,IY), IX=(IREC-1)*256+1,IREC*256)
          ENDDO
        ENDDO
C
C       Find max and min of array
        MIN = 32767
        MAX = INDATA(256,257)
        DO IY = 1,IMSIZE
```

```
          DO IX = 1,IMSIZE
            IF (INDATA(IX,IY) .LT. MIN) THEN
              MIN = INDATA(IX,IY)
            ELSEIF (INDATA(IX,IY) .GT. MAX) THEN
              MAX = INDATA(IX,IY)
            ENDIF
          ENDDO
        ENDDO
        MAXI4 = MAX
        MINI4 = MIN
C
C       Find radii and sum up, with peak normalized to 1
        ICX = IMSIZE/2
        ICY = ICX+1
        SCALE = 1./FLOAT(MAXI4 - MINI4)
        DO IY = 1,IMSIZE
          DO IX = 1,IMSIZE
            RADIUS = SQRT(FLOAT( (IX-ICX)**2 + (IY-ICY)**2))
            IBIN = RADIUS + 1
            POWER(IBIN) = POWER(IBIN) + (INDATA(IX,IY)-MINI4)*SCALE
            IWEIGHT(IBIN) = IWEIGHT(IBIN) + 1
          ENDDO
        ENDDO
C
C
C       Write into output file a single vector
        WRITE (11,1002) (POWER(IX),IWEIGHT(IX), IX=1,IMSIZE)
C
        CLOSE (UNIT=11)
        CLOSE (UNIT=10)
        CLOSE (UNIT=12)
        STOP
C
   99   STOP 'Error: end of input'
C
 1000   FORMAT(A)
 1001   FORMAT(A,A)
 1002   FORMAT (512(F10.6,I10/))
        END
```

IV. Mirror Pogram

This program finds the beam for an aperture of specified size at a given wavlength.

```
PRO MIRROR,INMAP,OUTMAP,DIAM,FOV
;       This procedure corrects the beam pattern (INMAP) for the finite
;       size in cm (DIAM) of the elemental mirrors.
;       The input (and output) maps have a field of view = FOV
;
;       Find the array size using the input array
        NS = SIZE(INMAP)
        IF (NS(0) LT 2) THEN GOTO,DIMERR        ;If not 2-D array
        IF (NS(1) NE NS(2)) THEN GOTO,DIMERR    ;flag a dimension error
        MAX  = NS(1)
        CENT = MAX/2 - 1                        ;This is the center
;                                               because IDL counts from zero
        CX = CENT
        CY = CENT + 1
        OUTMAP = FLTARR(NS(1),NS(2))            ;Creat the output array
;
; The wavelength is fixed at 500 nanometers = 0.5umeter
        C = 1.25664E5 * DIAM                    ;DIAM is in cm
;
; The constant SI is the FOV (mas) expressed in pixels
;               4.84814E-9 = 4.8E-6*E-3 for mas
        SI = 4.84814E-9 * FOV / 2.
        SI = SI / MAX
        CSI = C * SI
;
;       The output array is filled in one part and copied to reduce the
;       number of page faults on the VAX computer over what we would have
;       if the output array were filled directly.
        FOR J = 1,CY DO BEGIN
          FOR I = 0,J DO BEGIN
                ; First get the radial distance from the center = R
                R = SQRT(FLOAT((I-CX)^2 + (J-CY)^2))
                OUTMAP(I,J) = BESJ1(R * CSI) / (R*SI)   ;Calculate the
;                                               first order Bessel function
                OUTMAP(MAX-(I+2),J) = OUTMAP(I,J)    ;Use symmetry to store
          END
        END
        FOR J = 1,CY DO BEGIN
          FOR I = 0,J  DO BEGIN
                OUTMAP(MAX-(I+2),MAX-J) = OUTMAP(I,J)
                OUTMAP(I,MAX-J)     = OUTMAP(I,J)
          END
        END
        FOR J = 1,CY DO BEGIN
          FOR I = 0,J  DO BEGIN
                OUTMAP(J-1,I+1)     = OUTMAP(I,J)
                OUTMAP(MAX-(J+1),I+1)=OUTMAP(I,J)
```

```
          END
        END
        FOR J = 1,CY DO BEGIN
          FOR I = 0,J  DO BEGIN
                OUTMAP(MAX-(J+1),MAX-(I+1))=OUTMAP(I,J)
                OUTMAP(J-1,MAX-(I+1))=OUTMAP(I,J)
          END
        END
;       NOW WE MUST DO THE 4 SIDES FOR J=0
        FOR I = 0,CX DO BEGIN
                R = SQRT(FLOAT((I-CX)^2 + CY*CY))
                OUTMAP(I,0) = BESJ1(R*CSI) / (R*SI)
                OUTMAP(MAX-(I+2),0) = OUTMAP(I,0)
                OUTMAP(MAX-1,I+1)   = OUTMAP(I,0)
                OUTMAP(MAX-1,MAX-(I+1))=OUTMAP(I,0)
        END
        OUTMAP(CX,CY) = OUTMAP(CX+1,CY)
        OUTMAP = OUTMAP * OUTMAP
        OUTMAP = OUTMAP / OUTMAP(CX,CY)
        OUTMAP = OUTMAP * INMAP          ;Multiply the input map
RETURN
DIMERR:
        PRINT,'Input map is not square and at least 2-D'
        RETURN
END
```

END

FILMED

9-84

DTIC